RSC Advances

ROYAL SOCIETY OF CHEMISTRY

www.rsc.org/advances

Self-assembled Super-hydrophobic Multilayer Films with Corrosion Resistance on Copper Substrate

Ying Liu,[a,b] Huaijie Cao,[a] Yuanyuan Chen,[a] Shougang Chen,[a,*] Daoai Wang[b,*]

[a]*Institute of Material Science and Engineering, Ocean University of China, Qingdao 266100, China;*

[b]*Lanzhou Institute of Chemical Physics, Chinese Academy of Sciences, Lanzhou, 730000, China*

Corresponding email: wangda@licp.cas.cn; sgchen2009@ouc.edu.cn

Abstract

Micro and nano rough cube copper crystals were prepared on smooth copper substrate using simple electrodeposition method. 1–Dodecanethiol/polydopamine multilayer films were self-assembled layer-by-layer on modified rough copper surface. The surface contact angles of modified multilayer films could reach a maximum of about 154°, and the contact angles remained stable in air. A decrease in contact angle was observed after 35d of immersion in seawater. Electrochemical impedance spectroscopy result showed that the corrosion resistance and chemical stability of super-hydrophobic films were superior to the hydrophobic surface obtained in a previous study, and the modified functional surface exhibited corrosion resistance ability.

Keyword: Electrodeposition; Super-hydrophobic surface; Corrosion; Dopamine

1. Introduction

Wettability is a fundamental property for solid surfaces and plays an important role in daily life, industry, and agriculture. Inspired by the inherent “lotus effect”, extreme water repellency and super-hydrophobic surfaces[1,2] are due to the chemical coating with low surface-energy molecules and

surface roughness.[3–5] Artificial super-hydrophobic surfaces are popular among researchers for their benefits in functional textile production,[6–8] enhanced corrosion resistance,[9–12] anti-freeze and anti-snow properties, [13–15] bio-inspired aquatic materials, and devices field. [16, 17]

Recently, super-hydrophobic surfaces were fabricated by different methods on various engineering material surfaces, such as zinc, copper, steel, magnesium, and aluminum, to improve their corrosion resistance.[9–11, 18–22] Copper is an important metal and is widely used in heat exchangers, electrical power lines for communications, and pipelines for domestic and industrial water utilities. However, copper materials corrode easily when used, especially in an aqueous environment containing even trace amounts of Cl^-. In our past work, [9, 10] etched copper electrodes in acid solution have been used to fabricate n–tetradecanoic acid super-hydrophobic coating using the dip-coating method at the cost of sacrificing the mechanical properties of metal surfaces, thereby undermining corrosion resistance, weakening the adhesive force between the film and substrate, and leading to the easy exfoliation and rapid loss of corrosion resistance of super-hydrophobic film. To address these problems, dopamine-assisted 1–dodecanethiol complex film was selected to enhance the stability and corrosion resistance of copper surfaces on non-etching copper surfaces. Although the corrosion resistance of modified films in seawater improved, the corrosion resistance decreased quickly with increasing immersion time. Moreover, the contact angle only reached a maximum of about 120°. [23] Therefore, a method for increasing the contact angle for the protective film with good corrosion resistance and high stability is still required.

Generally, surface roughness and low surface energy materials are indispensable in super-hydrophobic surfaces.[24-26] A simple and time-saving potentiostatic electrolysis method is proposed to deposit micro and nano coppers on the substrate to increase its roughness. Structural analysis and surface wettability of the film are characterized by scanning electron microscopy (SEM), energy dispersive X-ray spectroscopy (EDS), X-ray photoelectron spectroscopy (XPS), and contact angle measurements. The corrosion resistance and durability of the super-hydrophobic coating on copper surface in 3.5 wt% NaCl solution are investigated using electrochemical impedance

spectroscopy (EIS) and contact angle measurements.

2. Experimental

2.1. Materials

Copper (≥ 99.5wt %) foils were mechanically abraded with SiC papers of different grit values (400, 600, 800, 1000, 1200, and 2000#) and polished with 0.5 μm diamond paste. These samples were then ultrasonically cleaned with acetone, ethanol, and distilled water for 5 min, and then dried with N_2 before treatment.

2.2. Copper surface modification

Micro- and nano-structured cube copper samples were grown in a two-electrode cell, where the copper samples acted as the cathode, and a platinum wire acted as the anode. The metallic copper films were grown on copper substrate at a voltage of -0.5 V, and $CuCl_2$ and Na_2SO_4 solutions at an appropriate ratio were used as electrolyte. The modified copper substrate was immersed in alkaline dopamine (DA) solution. After 24 h, the substrate was removed from the solution, rinsed with deionized water, and dried under N_2 gas flow. 1–Dodecanethiol (10 mM) was dissolved in dichloromethane for 1–dodecanethiol (SH) ad-layer formation. Before the formation of 1–dodecanethiol film, the oxygen in the solution was removed by bubbling with N_2, and the polydopamine-coated copper substrate was added. The substrate was removed after 24 h, and the film was rinsed by ethanol and dried under N_2 flow. For comparison, the DA and DA-SH films were prepared on smooth copper surface under the same conditions, including the same immersion time and procedures.

2.3. Measurements

The phase content was determined by X-ray diffraction (XRD) with a Rigaku D/max 2550 VB/PC apparatus at room temperature using Cu Ka1 radiation (k = 1.5406 Å). The morphology of the

coatings were characterized by a field-emission SEM (FE-SEM, JEOL-JSM-6700F) at 5.0 kV, and chemical composition data of films on copper samples were characterized by EDS and XPS (PHI-5702 multifunctional spectrometer using Al Ka radiation).

Surface wettability was tested by the JC2000C1 system (provided by Shanghai Zhongchen Digital Technology Apparatus Co., Ltd.) at ambient temperature, and the volume of the test droplet is about 5 μL. At least five parallel positions on one surface were measured to attain the average values of the contact angles.

The electrochemical impedance spectroscopy (AUTOLAB 302N Electrochemical workstation, Switzerland) was used to explore the corrosion resistance of samples in 3.5 wt% NaCl solution at ambient temperature. The experiment was performed in a three-electrode cell system with a platinum auxiliary electrode as a counter electrode (CE), a bare copper sheet or super-hydrophobic copper sheet with an exposure surface of 10 mm × 10 mm as a working electrode, and a saturated calomel electrode (SCE) as a reference electrode. Electrochemical impedance spectroscopy (EIS) measurements were performed at a frequency range of 100 kHz to 10 mHz at open circuit potential (OCP) with amplitude of perturbation voltage ±10 mV.

3. Results and discussion

SEM and contact angle images (Fig. 1) show that the cube-shaped copper grew randomly on the polished copper sample. The nanoscale cube-shaped copper and some smaller scale copper particles presented a hierarchical structure (Fig. 1b), and the corresponding XRD pattern (Fig. 1f) confirmed the as-grown pure cube copper crystal. The polished copper sample was very smooth except for some cracks, and its contact angle was about 71° (Fig. 1e). The contact angle of the as-depositing copper surface decreased to 47°, and this decrease was attributed to the rough cube copper crystal nanostructure on the surface. This phenomenon complies with the Wenzel equation.[28-29] However, the contact angle of the DA-SH modified pre-depositing copper substrate reached 154°, and the signals of C, O, and S elements also indicated that the DA-SH film was formed on the pre-depositing copper

surface (Fig. 1g). Micro-nano rough cube copper crystal surface and low surface energy chemical modification were essential for fabricating the super-hydrophobic surface (Fig. 1c).

After the super-hydrophobic film was successfully fabricated on rough nanostructure copper surface, researchers determined the long-term stability and corrosion-resistant performance of the film immersed in 3.5 wt% NaCl solution. EIS technology was applied to studying the corrosion resistant phenomenon. The electrochemical impedance spectra for different copper electrodes immersed in 3.5 wt% NaCl solution contained a depressed semicircle with the center under the real axis (Fig. 2), which is a characteristic behavior of solid electrodes and is often referred to as frequency dispersion; frequency dispersion is attributed to the roughness and other inhomogeneities of the solid electrode. [30] The Nyquist diagrams (Fig. 2a) show that the diameter of the capacitance looping with super-hydrophobic film was larger than the DA and DA-SH films on the smooth copper surface, thereby suggesting that the super-hydrophobic film has good corrosion resistance in 3.5 wt% NaCl solution.[10] In our past work, the Z modulus (Fig. 2b) of the DA-SH film only reached 10^5 Ωcm^2 at low frequency, [23] whereas the Z modulus of the super-hydrophobic film reached $10^{6.5}$ Ωcm^2, indicating that the super-hydrophobic film has outstanding corrosion resistance. The air trapped in the surface acts as a barrier and prevents corrosive ions from penetrating the copper substrate. The type of super-hydrophobic films fabricated in this study was more beneficial compared with the previously studied etched method.[10] Our films showed high corrosion resistance ability and good interfacial adhesive force.

The anti-corrosion ability of DA-SH super-hydrophobic coatings was evaluated by the measurement of potential dynamic polarization curve in 3.5 wt% NaCl solution, as shown in Fig. 3. DA-SH super-hydrophobic coatings present more positive corrosion potential (E_{corr} is -0.296V vs. SCE) and lower current density (I_{corr} is $1.02\times10^{-8}A\cdot cm^{-2}$) during the process of cathode or anode polarization than the bare copper specimen.

Time constants for the blank copper substrate, DA coating, DA-SH coating and the

super-hydrophobic coating can be determined from Bode-phase angle versus frequency plots (Fig. 2c). The blank copper shows one time constant and low phase angle in high frequency zone. After coating modification, the specimens display high phase angle in high frequency zone. The super-hydrophobic coating shows a wider platform from high frequency zone to medium frequency zone, which is in accord with the results of Fig. 2a.

The inhibition efficiency (η_P) was calculated by the following equation 1, [31–33]

$$\eta_P\% = \frac{(i_{corr}^0 - i_{corr})}{i_{corr}^0} \times 100 \qquad (1)$$

Table 1 shows the electrochemical kinetic parameters obtained by potentiodynamic polarization curves. As shown in Table 1, the existence of the films reduced both the anodic and cathodic currents, and a significant positive shift for the corrosion potential was observed. Thus, the coverage of the films reduced the corrosion rate of the bare copper, especially for the substrate with DA-SH super-hydrophobic coating. The η_P values of the DA-SH Superhydrophobic film can reach 99.89.

Based on previous reports, [9,10] super-hydrophobic surface composed of hills could easily bring about large amounts of air trappings within the "valleys" between the hills, and the Cl^- could hardly contact the bare surface, which agreed well with the SEM results (Fig. 1c). Contact angle maintainability in corrosive solution for the super-hydrophobic surface plays an increasingly vital role in practical application. The changes of contact angles for the super-hydrophobic surface exposed in air and immersed in 3.5 wt% NaCl solution with increasing time are shown in Fig. 4. The average contact angle of the modified surface hardly fluctuated in air. In 3.5 wt% NaCl solution, the contact angle decreased from 154° to 150° after 5 d, and the contact angle decreased to 144° after immersion for 10 d. With increasing immersion days (until 35 d), the contact angle continuously decreased to 138°, but it was still larger than the result in a previous study. [23] Owing to the replacement of air trapped in the film by water, the air trapped in the rough structures reduced, and the contact angles of the superhydrophobic film decreases continuously with immersion time. [34]

The Bode plots for bare copper and modified super-hydrophobic surface immersed in 3.5 wt% NaCl solution for different days are shown in Fig. 5. Initially, the super-hydrophobic film exhibited high corrosion resistance because of its dense structure with only a few cracks (Figs. 1c and 1d). After 5 d, two time constants were observed from high, medium, to low frequency field (Fig. 5b). The time constant of the high-frequency area could be attributed to the outermost film, whereas the small tail below 0.1 Hz was ascribed to the copper surface.[30, 35–36] On the one hand, the capacitive loops at high frequencies decreased gradually with increasing immersion time, which revealed that the film slightly dissolved in NaCl solution. On the other hand, a time constant at 0.1 Hz was formed (Fig. 5b) after 5 d of immersion, thereby showing that the initially produced micro and nano rough copper surfaces were slightly pitted. The impedance also decreases continuously over the 35 days - at the lowest frequency recorded (10 mHz), the value of |Z| decreases by more than an order of magnitude (Fig 5). After 35 days it is about 1 order of magnitude above that of the bare copper. While, after 35 d of immersion, the corrosion resistance of the modified super-hydrophobic surface was still greater than that of bare copper (Fig. 5a), as well as the previous result for 1 d immersion.[10] Compared with previous hydrophobic DA-SH films, the electrochemical results of the super-hydrophobic surface after 35 d of immersion nearly had the same corrosion resistance as in previous hydrophobic DA-SH films after 1 d of immersion,[23] suggesting that the super-hydrophobic film fabricated in this study can effectively protect the surface from corrosion.

Equivalent circuit models of the different samples are shown in Fig. 6. In electrochemical fit, constant phase angle element (CPE) is typically used to replace pure capacitance. In this circuit, R_{ct} is the charge transfer resistance, R_s is the solution resistance, R_f is the film resistance, CPE_f values are the constant phase elements of the film, and CPE_{dl} is the electrical double layer. Value of R_{ct} directly indicates anti-corrosion ability. R_{pit} and CPE_{pit} represent resistance and the constant phase element of the oxidation corrosion product layer, respectively. The equivalent circuit model in Fig. 6(a) was used to fit the EIS data of pure copper in 3.5 wt% NaCl aqueous solution for 30 min. After adsorption of

super-hydrophobic coating on copper substrate, the equivalent circuit model in Fig. 6b was used to fit the EIS data. After immersion in the 3.5 wt% NaCl aqueous solution for 15 d, the super-hydrophobic film shows an obvious time constant in low frequency range, and appearance of the time constant is mainly due to slight corrosion occurring in the copper substrate surface, which resulted in the formation of an oxidation layer (Fig. 5b). Thus, we used the equivalent circuit model in Fig. 5c to fit the EIS data of super-hydrophobic surface after immersion in 3.5 wt% NaCl aqueous solution for different days. The electrochemical parameters listed in Table 2 indicate that the super-hydrophobic film (SH-Cu) has low capacitance (CPE_f and CPE_{dl}) and high resistance (R_f and R_{ct}), thereby proving that super-hydrophobic films effectively protect the copper substrate from corrosion. With increasing immersion time, both the capacitance (CPE_f and CPE_{dl}) and the resistance (R_f and R_{ct}) of the super-hydrophobic film decreased, but the film still played a protective role for the substrate.

The OCP changes of the coated film were shown in Fig.7. The OCP of the coated sample shifted to more positive direction with the immersion time. After 35 days, the OCP reached to -0.232V(vs. SCE). All this suggests that the formation of oxide film and accumulation of corrosion products on the copper surface, which inhibits the oxidation process.[37] Also accumulation of corrosion products on the film was partly protective to the substrate.

Changes of film resistance and charge transfer resistance with immersion time were shown in Fig.8. From Fig.8(a), the R_f increased with the immersion time owing to the formation of corrosion products and adsorption of medium ions in this organic film. And then it started to decrease because of the destruction of the organic film. As shown in Fig. 8(b), the R_{ct} of the film reduced with the immersion time for 15 days. So the protection efficiency of the film declined as the immersion time. It can be seen that the R_{ct} value increases after immersion for 25 days, which might be ascribed to the accumulation of corrosion product over film during immersion.[38] With the destruction of the film, the R_{ct} value

decreases after immersion for 35 days. The R_f of the film after immersion for 35 days was still higher than that of the bare copper, and the R_{ct} still remained 15.3 kΩ cm^2. So after immersion for 35 days, the corrosion resistance decreased indeed, but the film could still provide protective ability on copper substrate. The hydrophobicity of the film decreased over immersion time, so the permeability of the film increased, Cl^- ions in NaCl solution can penetrate the DA-SH organic coating and interact with substrate, and corrosion products were retained in the pores of the coating. A loose layer formed and the protective property decayed. [39] Even so, the hydrophobicity of the film decreased over immersion time, so the permeability of the film increased, Cl^- ions in NaCl solution can penetrate the DA-SH organic coating and interact with substrate, and corrosion products were retained in the pores of the coating. The decrease of corrosion resistance may be attributed to ionic penetration in the hydrophobic layer. [40] So the coating would be destructed with long immersion time, so the protection decayed.

4. Conclusions

Pure cube-shaped copper film was fabricated on a copper surface using the electrodeposition method, and the DA-SH film was self-assembled layer by layer on the pre-deposition copper surface. The film presented super-hydrophobicity with a contact angle of 154°. The super-hydrophobicity of the film is ascribed to micro and nano rough cube copper crystal structures and low surface energy chemical modification of DA-SH. The corrosion resistance of the super hydrophobic film formed on copper surface in 3.5 wt% NaCl solution was investigated by the EIS techniques and potentiodynamic polarization test. The electrochemical results show that the super-hydrophobic film exhibits a high Z modulus at low frequency and low corrosion current density, indicating that it can prevent the copper substrate from corroding. Moreover, the corrosion resistance of the super-hydrophobic film is also related to its water repellent property. The contact angle of the super hydrophobic surface keeps above 150° in air after 35 d, with a slight decrease to 138° after immersion in 3.5 wt% NaCl solution for 35 d. EIS results of the super-hydrophobic film after 35 d of immersion in 3.5 wt% NaCl aqueous solution

showed that the film can provide corrosion protection for copper substrate. This corrosion resistance for the super-hydrophobic film is attributed to its water repellent property. The entire preparation process is simple and environment friendly, and this method could enhance the corrosion resistance of copper.

Acknowledgments

This work was sponsored by the National Nature Science Foundation of China (NSFC, 21203171, 51572249) and China postdoctoral science foundation of the fifty-sixth batch of funds (2014M561965).

References

1. A. Hozumi, O. Takai, *Thin Solid Film,*1997, **303**, 222-225.

2. K. Takeda, M. Sasaki, N. Kieda, K. Katayama, T. Kako, K. Hashimoto, T. Watanabe, A. Nakajima, *J. Mater. Sci. Lett.,* 2001, **20**, 2131-2133.

3. K. Azumi, N. Yasui, M. Seo, *Corros Sci.,* 2000, **42**, 885-896.

4. H.B. Wang, Q.M. Pan , J.W. Zhao, G.P. Yin, P.J. Zuo, *J. Power Sources,* 2007, **167**, 206-211.

5. J. L. Song, W. J. Xu, Y. Lu, X. Liu and J. Sun, *Mater. Corros.*, 2013, **64**, 979-987.

6. J. Vince, B. Orel, A. Vilcnik, M. Fir, A.S.Vuk, V. Jovanovski, B. Simončič, *Langmuir*, 2006, **22**, 6489-6497.

7. M.H. Yu, G.T. Gu, W.D. Meng, F. L. Qing, *Appl. Surf. Sci.* 2007, **253**, 3669-3673.

8. T. Bahners, T. Textor, K. Opwis and E. Schollmeyer, *J. Adhes. Sci. Technol.* 2008, **22**, 285-309.

9. T. Liu, S.G. Chen, S. Cheng, J.T. Tian, X.T. Chang, Y.S. Yin, *Electrochim. Acta,* 2007, **52**, 8003-8007.

10. T. Liu, Y.S. Yin, S.G. Chen, X.T. Chang, S. Cheng, *Electrochim. Acta* 2007, **52**, 3709-3713.

11. T. Ishizaki, Y. Masuda, M. Sakamoto, *Langmuir* 2011, **27**, 4780-4788.

12. P.M. Barkhudarov, P.B. Shah, E.B. Watkins, D.A. Doshi, C.J. Brinker, J. Majewski, *Corros. Sci.*

2008, **50**, 897-902.

13. V. F. Petrenko, S. Peng, *Can. J. Phys.* 2003, **81**, 387-393.
14. M. He, J.X. Wang, H.L. Li, X.L. Jin, J.J. Wang, B.Q. Liu, Y. L. Song, *Soft Matter*., 2010, **6**, 2396-2399.
15. S.A. Kulinich, M. Farzaneh, *Appl. Surf. Sci*., 2009, **255**, 8153-8157.
16. F. Shi, Z.Q. Wang, X. Zhang, *Adv. Mater*. 2005, **17**, 1005-1009.
17. Q.M. Pan, M. Wang, *ACS Appl. Mater. Interfaces*, 2009, **1**, 420-423.
18. B. Qian, Z. Shen, *Langmuir* 2005, **21**, 9007-9009.
19. M. Qu, B. Zhang, S. Song, L. Chen, J. Zhang, X. Cao, *Adv. Funct. Mater.* 2009, **17**, 593-596.
20. T. He, Y. Wang, Y. Zhang, Q. Iv, T. Xu, T. Liu, *Corros. Sci.* 2009, **51**, 1757-1761.
21. M. Thieme, H.J. Worch, *Solid State Electrochem.* 2006, **10**, 737-745.
22. S.T. Wang, L. Feng, L. Jiang, *Adv. Mater.* 2006, **18**, 767-770.
23. S.G. Chen, Y. Chen, Y.H. Lei, Y.S. Yin, *Electrochem. Commun.* 2009, **11**, 1675-1679.
24. P. Wang, R. Qiu, D. Zhang, Z. F. Lin, B. R. Hou, *Electrochimi. Acta* 2010, **56**, 517–522.
25. Y. B. Zhou, Y. Yang, W. M. Liu, Q. Ye, B. He, Y. S. Zou, P. F. Wang, X. J. Pan, W. J. Zhang, I. Bello and S. T. Lee, *Appl. Phys. Lett.* 2010, **97**, 133110 -133112.
26. P. Wang, D. Zhang, R. Qiu, *Corros. Sci.*, **2011**, 53, 2080-2086.
27. P. Wang, D. Zhang, R. Qiu, J. Wu, Y. Wan, *Corros. Sci.,* **2013**, 69, 23-30.
28. R. N. Wenzel, *Ind. Eng. Chem.*, **1936**, 28, 988-994.
29. G. Wolansky, A. Marmur, *Colloids Surf. A*, **1999**, 156, 381-388.
30. G. L. Song, *Electrochim. Acta* 2010, **55**, 2258-2268.
31. X. P. Ouyang, X. Q. Qiu, H. M. Lou, D. J. Yang, *Ind. Eng.Chem. Res*. 2006, **45**, 5716-5721.
32. D. Daoud, T. Douadi, S. Issaadi, S. Chafaa, *Corros. Sci.* 2014, **79**, 50–58.

33 Y. Liu, S. Li, J. Zhang, J. Liu, Z. Han, L. Ren, *Corros. Sci.* 2015, **94**, 190-196.

34. P. Wang, D. Zhang, R. Qiu, J.J. Wu, *Corros. Sci.* 2014, **83**, 317-326.
35. S. Feliu, J.C. Galvan, M. Morcillo, *Corros. Sci.* 1990, **30**, 989-998.

36. D.Q. Zhu, W.J. van. Ooij, *Corros. Sci.* 2003, **45**, 2177-2197.

37. R. Fuchs-Godec, G. Zerjav, *Corros. Sci.* 2015, **97**, 7–16.

38. P. Wang, Z. Lu, D. Zhang, *Corros. Sci.* 2015, **93**, 159–166.

39. X.J. Cui, X.Z. Lin, C.H. Liu, R.S. Yang, X.W. Zheng, M. Gong, *Corros. Sci.* 2015, **90**, 402–412.

40. G. Zerjav, I.Milosev, Corros. Sci. 2015, **98**, 180–191.

Table Captions

Table 1 Electrochemical kinetic parameters obtained by potentiodynamic polarization curves for different copper electrodes in 3.5 wt% NaCl aqueous solution at room temperature.

Table 2 Electrochemical parameters obtained from fitting results of EIS plots from Fig. 5.

Figure Captions

Fig. 1 SEM images of (a) cube-shaped copper film modified surface. (b) Magnified image on a single region of a. (c) DA-SH modified surface. (d) Amplified diagram of super-hydrophobic surface. (e) Bare copper surface. (f) The corresponding XRD analysis of b. (g) The corresponding EDS analysis of c. The insets are the contact angle photographs of water droplets covering the surfaces.

Fig. 2 The EIS results for unmodified, differentially treated copper samples in 3.5 wt% NaCl aqueous solution: (a) Nyquist plot, (b) Bode plots and (c) Bode-phase angle versus frequency plots. The insets are the enlarged impedance spectra in the higher frequency range.

Fig. 3 Potentiodynamic polarization curves for different copper surfaces in 3.5 wt% NaCl aqueous solution after immersion for 30 minutes.

Fig. 4 Changes in contact angle of the super hydrophobic surface after exposure in air and immersion in 3.5 wt% NaCl aqueous solution for different days.

Fig. 5 Bode plots of modified copper samples during immersion in 3.5 wt% NaCl aqueous solution for different days; (a) impedance plot and (b) phase angle plot.

Fig. 6 Equivalent circuit models for (a) bare copper surface (b) super-hydrophobic surface after immersion in 3.5 wt% NaCl solution for 30 min (c) super-hydrophobic surface after immersion in 3.5 wt% NaCl aqueous solution for different days.

Fig.7 OCP changes of the superhydrophobic film versus the immersion time

Fig. 8 Changes of R_f film resistance(a) and R_{ct} charge transfer resistance(b) of the superhydrophobic film versus immersion time

Table 1

Samples	$-\beta_c$ (V/dec)	β_a (V/dec)	E_{corr} (V/SCE)	I_{corr} ($\mu A \cdot cm^{-2}$)	CR (10^{-5}mm/a)	η_P (%)
Cu	0.413	0.157	-0.478	9.33	275.436	—
Cu+DA	0.144	0.137	-0.333	2.12	62.5145	77.28
Cu+DA+SH	0.081	0.100	-0.453	0.368	10.8509	96.06
Cu+Cu+DA+SH	0.046	0.037	-0.296	0.0102	0.30226	99.89

Table 2

Samples	Rs (Ω cm^2)	R_f (kΩ cm^2)	CPE_f $Y_f(\Omega^{-1}$ s^n cm^{-2})	n_f	CPE_{dl} $Y_{dl}(\Omega^{-1}$ s^n cm^{-2})	n_{dt}	R_{ct} (kΩ cm^2)	CPE_{pit} $Y_{pit}(\Omega^{-1}$ s^n cm^{-2})	n_{pit}	R_{pit}
Bare Cu	17.4	5.86	6.90×10^{-6}	0.942	-	-	-	-	-	-
SH-Cu	15.0	9.88	2.76×10^{-8}	0.823	5.43×10^{-8}	0.687	3391	-	-	-
SH-Cu-35d	17.8	6.58	5.22×10^{-7}	0.412	3.21×10^{-6}	0.615	15.3	2.69×10^{-5}	0.534	276

Fig. 1

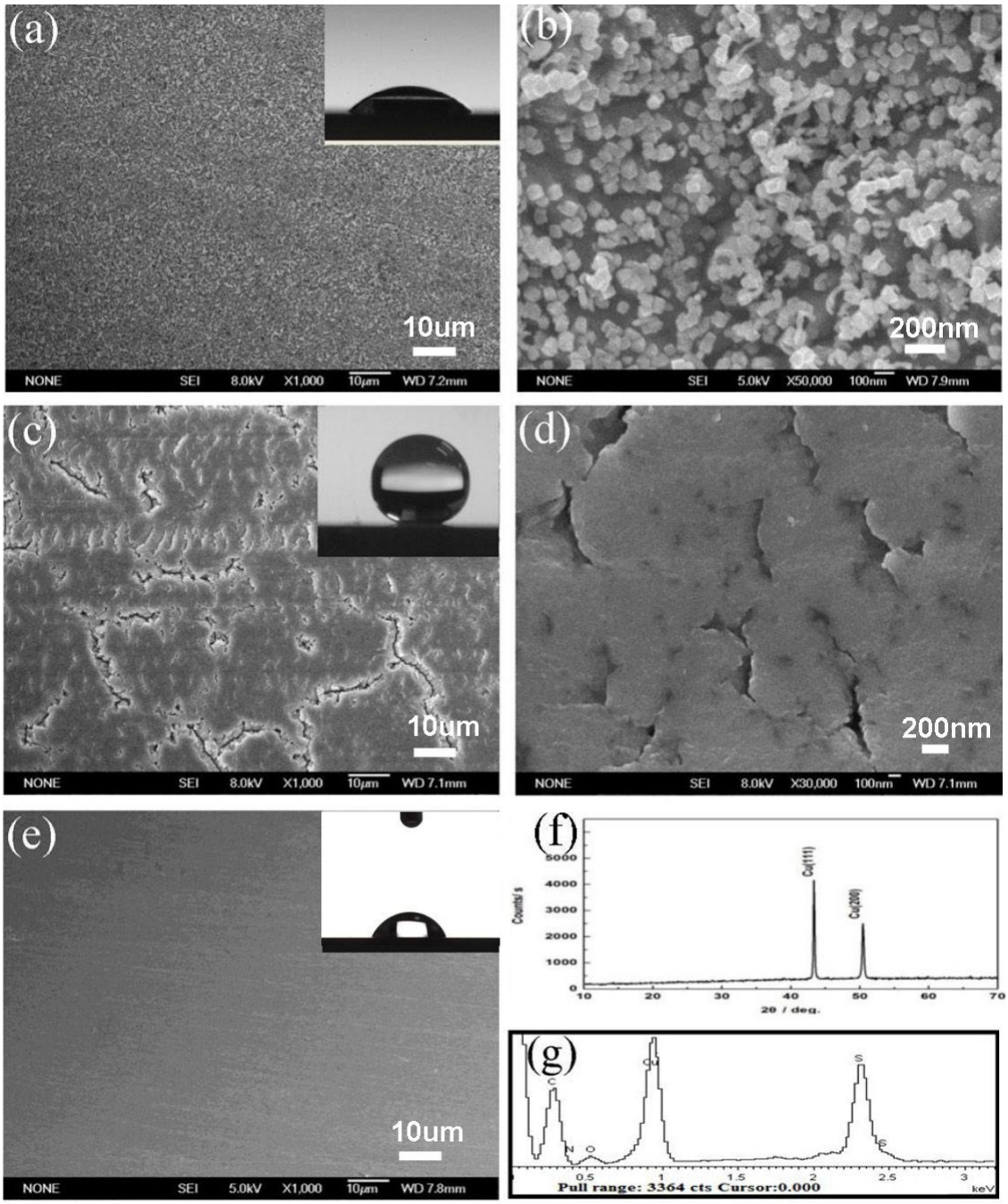

Fig. 2

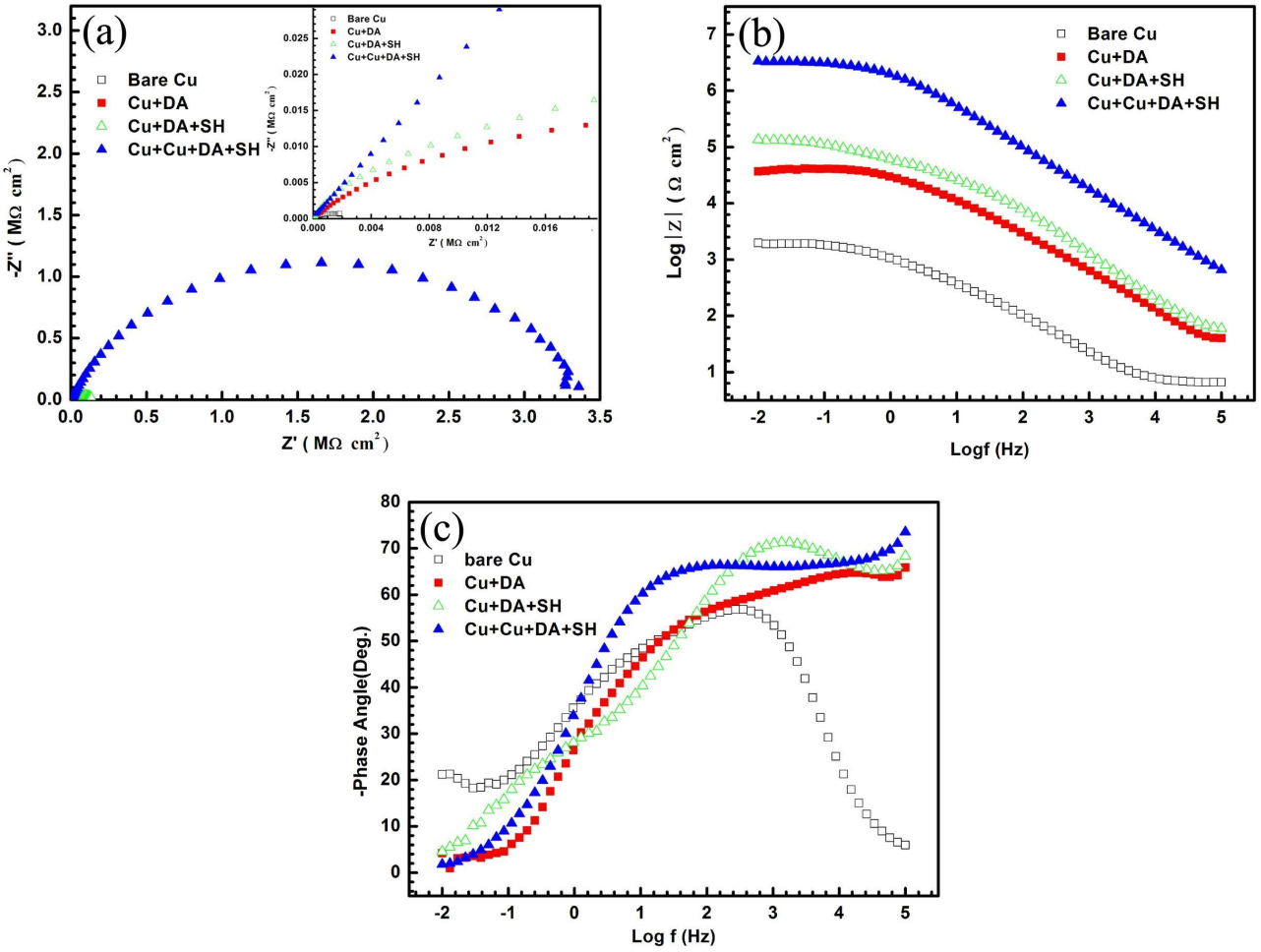

Fig. 3

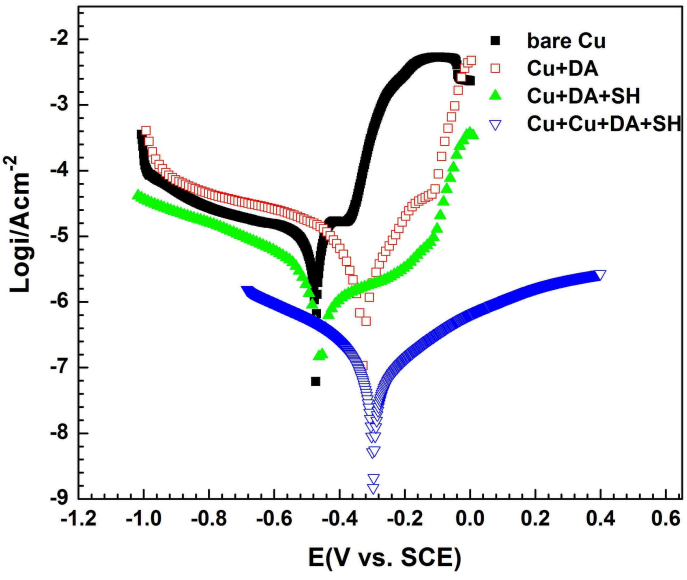

Fig. 4

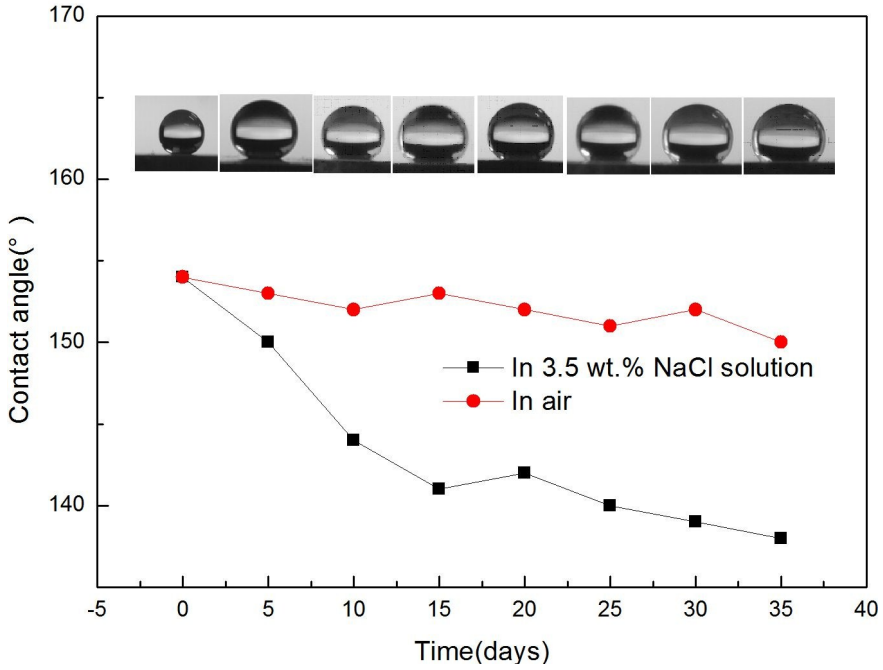

Fig. 5

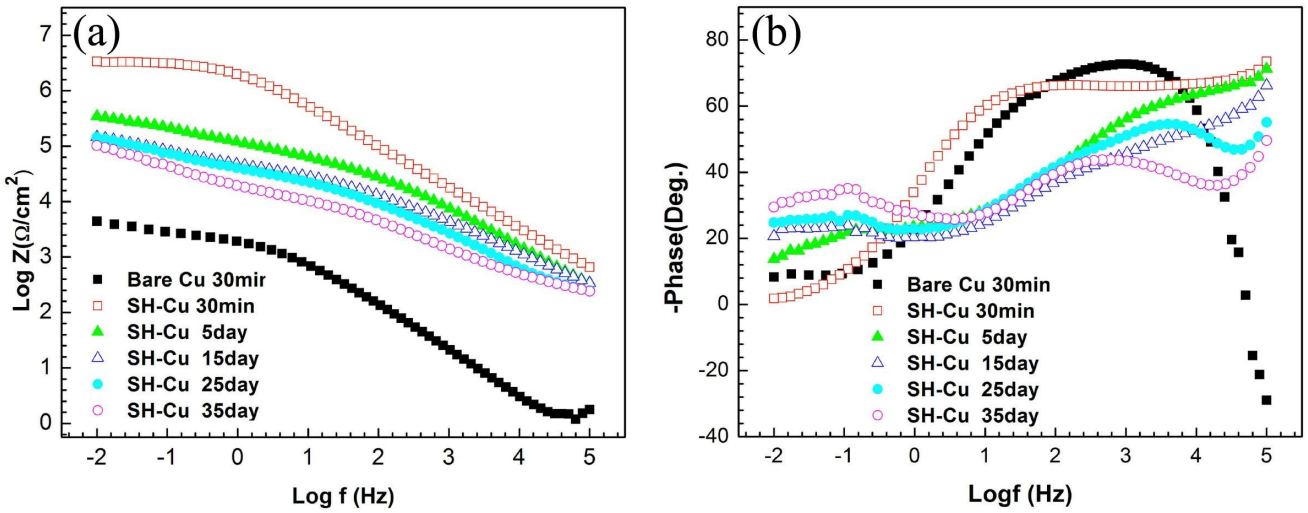

Fig. 6

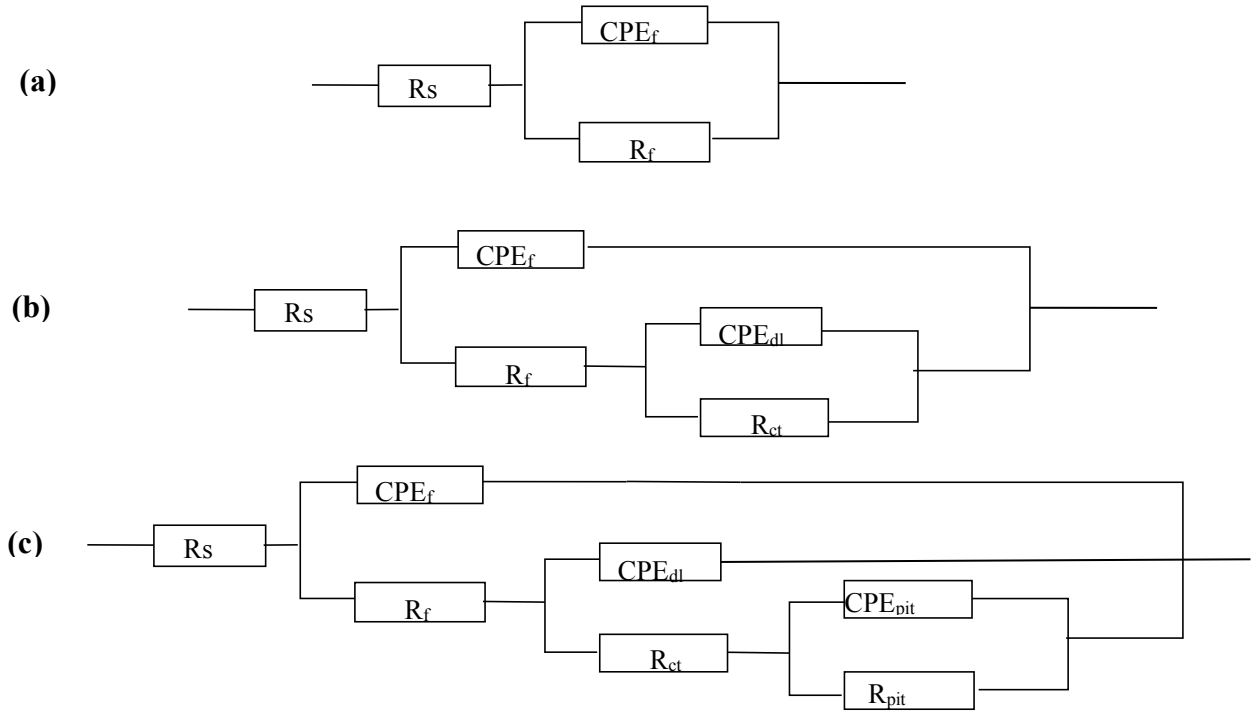

Fig. 7

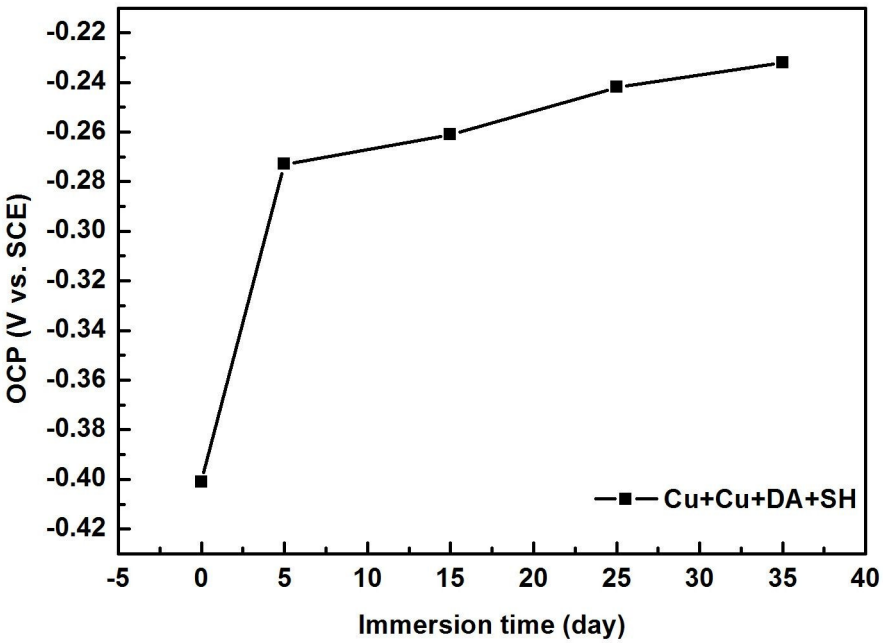

Fig. 8

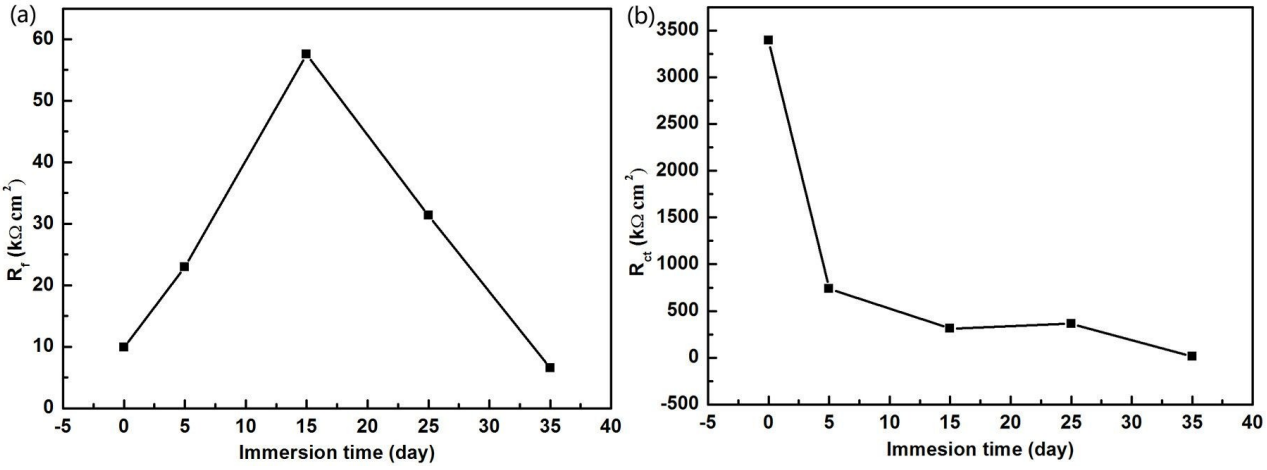

Micro and nano rough cube copper crystals were prepared on smooth copper substrate using simple electrodeposition method. 1–Dodecanethiol/polydopamine multilayer modified films were self-assembled layer-by-layer on modified rough copper surface. The surface contact angles of modified multilayer films reached a maximum of about 154°, and the contact angles remained stable in air. A decrease in contact angle was observed after 35d of immersion in seawater. Electrochemical impedance spectroscopy result showed that the corrosion resistance and chemical stability of super-hydrophobic films were superior to the hydrophobic surface obtained in a previous study, and the modified functional surface exhibited corrosion resistance ability.

TOC Figure